



## Research article

# Establishment of novel anti-TIM-3 antibodies interfering with its binding to ligands

Zhuohong Yan<sup>a,\*</sup>, Teng Ma<sup>a,1</sup>, Xiaojue Wang<sup>a</sup>, Ling Yi<sup>a</sup>, Panjian Wei<sup>a</sup>,  
Hongtao Zhang<sup>a</sup>, Jinghui Wang<sup>a,b,\*\*</sup>

<sup>a</sup> Cancer Research Center, Beijing Chest Hospital, Capital Medical University, Beijing Tuberculosis and Thoracic Tumor Research Institute, Beijing, 101149, China

<sup>b</sup> Department of Medical Oncology, Beijing Chest Hospital, Capital Medical University, Beijing Tuberculosis and Thoracic Tumor Research Institute, Beijing, 101149, China

## ARTICLE INFO

## Keywords:

TIM-3  
Galectin-9  
Monoclonal antibody  
HMGB-1  
CEACAM-1  
Conformational epitope

## ABSTRACT

The T cell immunoglobulin and mucin-domain containing-3 (TIM-3) receptor has gained significant attention as a promising target for cancer immunotherapy. The inhibitory effect of T cells by TIM-3 is mediated through the interaction between TIM-3 and its ligands. Ligand-blocking anti-TIM-3 antibodies possess the potential to reactivate antigen-specific T cells and augment anti-tumor immunity. However, the precise ligand-receptor interactions disrupted by the administration of TIM-3 blocking Abs have yet to be fully elucidated. In this study, we have developed a panel of monoclonal antibodies targeting human TIM-3, namely MsT001, MsT065, MsT229, and MsT286. They exhibited high sensitivities (10 pg/mL) and affinities ( $3.70 \times 10^{-9}$  to  $4.61 \times 10^{-11}$  M) for TIM-3. The TIM-3 antibodies recognized distinct epitopes, including linear epitopes (MsT001 and MsT065), and a conformational epitope (MsT229 and MsT286). Additionally, the MsT229 and MsT286 displayed reactivity towards cynomolgus TIM-3. The interactions between TIM-3/Gal-9, TIM-3/HMGB-1, and TIM-3/CEACAM-1 disrupt the binding of MsT229 and MsT286, while leaving the binding of MsT001 and MsT065 unaffected. The inhibitory effect on the interaction between Gal-9 and TIM-3 was found to be dose-dependently in the presence of either MsT229 or MsT286. The findings suggested that the involvement of conformational epitopes in TIM-3 is crucial for its interaction with ligands, and we successfully generated novel anti-TIM-3 Abs that exhibit inhibitory potential. In conclusion, our finding offers valuable insights into the comprehension and targeting of human TIM-3.

## 1. Introduction

The utilization of immune checkpoint inhibitors (ICIs) has become an indispensable cornerstone in the field of cancer therapy. Numerous patients with a broad variety of hematological and solid malignancies now have better prognoses due to ICIs that target

\* Corresponding author. Cancer Research Center, Beijing Chest Hospital, Capital Medical University, Beijing Tuberculosis and Thoracic Tumor Research Institute, No. 97 Machang, Tongzhou District, Beijing, 101149, China.

\*\* Corresponding author. Cancer Research Center, Beijing Chest Hospital, Capital Medical University, Beijing Tuberculosis and Thoracic Tumor Research Institute, No. 97 Machang, Tongzhou District, Beijing, 101149, China.

E-mail addresses: [yanzhuohong@bjxkyy.cn](mailto:yanzhuohong@bjxkyy.cn) (Z. Yan), [jinghuiwang2006@163.com](mailto:jinghuiwang2006@163.com) (J. Wang).

<sup>1</sup> These authors contributed equally.

<https://doi.org/10.1016/j.heliyon.2024.e28126>

Received 24 October 2023; Received in revised form 12 March 2024; Accepted 12 March 2024

Available online 18 March 2024

2405-8440/© 2024 The Authors. Published by Elsevier Ltd. This is an open access article under the CC BY-NC-ND license (<http://creativecommons.org/licenses/by-nc-nd/4.0/>).

lymphocyte-activation gene 3 (LAG-3), cytotoxic T lymphocyte-associated protein 4 (CTLA-4), programmed cell death 1 (PD-1), and its ligand PD-L1. However, for most patients with common cancers, their clinical response and efficacy have been limited. This suggests that in order to increase response rates of currently available immunotherapeutic drugs, it may be necessary to further exploit additional inhibitory receptors. As a result, more and more immunotherapeutic agents are being investigated, such as TIGIT [1], CD73/A2aR [2], CD70 [3], OX40 [4], and TIM-3 [5].

TIM-3 (also known as HAVCR2) represents a promising target for cancer immunotherapy due to its co-inhibitory receptor properties [5–9]. TIM-3 was initially discovered on CD4<sup>+</sup> T helper (Th) 1 and cytotoxic CD8<sup>+</sup> T cells that secreted interferon (IFN)  $\gamma$  [10]. Moreover, Th17 cells [11], regulatory T cells [12], dendritic cells [13], macrophages [10], and activated natural killer (NK) cells [14] express it. TIM-3 plays crucial roles in the regulation of both innate and adaptive immune responses. Upon binding to its ligand, TIM-3 effectively suppresses the responses of T cells and NK cells, which helps tumor cells evade immune surveillance [15,16]. There are four TIM-3 ligands being reported: galectin-9 (Gal-9) [17], phosphatidylserine (PtdSer) [18], high-mobility group box 1 protein (HMGB-1) [13], and carcinoembryonic antigen-related cell adhesion molecule 1 (CEACAM-1) [19].

TIM-3 is a well-established marker linked to T cell exhaustion. Poor outcomes and tumor progression have been correlated to elevated levels of TIM-3 expression on CD8<sup>+</sup> T cells [20,21]. The co-expression of TIM-3 and PD-1 is frequently observed on tumor-infiltrating CD8<sup>+</sup> T cells. When compared to PD-1<sup>+</sup>Tim-3<sup>-</sup>CD8<sup>+</sup> T cells, PD-1<sup>+</sup>Tim-3<sup>+</sup>CD8<sup>+</sup> TILs exhibit the most severe exhaustive phenotype and suppressive function [21–24]. An increasing amount of research has demonstrated that TIM-3 expression is upregulated by PD-1 inhibition in various cancers and that TIM-3 expression is closely correlated with resistance to both primary and secondary PD-1 blockade [25–28]. Combination therapy that blocking both TIM-3 and PD-1 have been shown to have synergistic effects, including the restoration of T-cell responses in vitro and the induction of anti-tumor responses in preclinical animal models [21, 29]. Additionally, TIM-3 blockade indirectly supports the effector function of CD8<sup>+</sup> T cells by regulating the functionality of intratumoral conventional dendritic cells (cDC) [6,30].

Currently, several monoclonal antibodies (mAbs) targeting TIM-3, such as MBG453, TSR-022, and Sym023, are undergoing early-phase clinical trials [5]. The combination of TIM-3 blockade and anti-PD-1/PD-L1 therapy is believed to hold significant potential in augmenting the efficacy of anti-PD-1/PD-L1 therapy and may overcome resistance to such treatment [31]. Clinical trials are currently investigating the combined blockade of TIM-3 and PD-1 in patients with various cancers. The global approval for any drug targeting TIM-3 is presently pending. However, the existing market necessitates a wider variety of TIM-3 antibodies to thoroughly investigate its functionality and facilitates antibody selection for subsequent companion diagnostic applications. We have successfully generated novel mAbs exhibiting exceptional sensitivity and affinity towards the human TIM-3 protein in this study, thereby holding potential for utilization in cancer immunodiagnosis and immunotherapy.

## 2. Materials and methods

### 2.1. Mouse immunizations

This study utilized two BALB/c mice, aged 6–8 weeks, which were purchased from Charles River. The mice were subcutaneously immunized with 100  $\mu$ g of TIM-3-His recombinant protein (ACRO Biosystems, Beijing, China; TIM3-H5229) emulsified in a 1:1 volume of complete Freund's adjuvant (Sigma). The mice were subsequently boosted with the same dose of TIM-3-His protein in an emulsion containing incomplete Freund's adjuvant every 3 weeks for a total duration of six months. Ab titers were measured in serum obtained from the orbital vein 7 days after the last boost immunization. The mouse with a higher Ab titer was subjected to intraperitoneal injection with 100  $\mu$ g TIM-3-His protein for final immunization. The mouse spleen was harvested and stored in liquid nitrogen on the third day after the final immunization.

### 2.2. Library generation and selection

We successfully generated rabbit anti-lipoarabinomannan mAbs in our earlier investigation by utilizing a phage display single-chain variable fragment (scFv) library [32]. In this study, we constructed a phage display scFv library using spleen cells from a mouse that had been immunized with human TIM-3-His protein. After spleen cells were collected, total RNA was extracted, and RT-PCR was used to create first-strand cDNA. Heavy chain variable region ( $V_H$ ) and light chain variable ( $V_L$ ) genes were amplified using PCR, then splicing overlap extension PCR was used to splice the amplified genes into a whole scFv gene. The PCR fragments obtained were subsequently inserted into the pComb3X phagemid vector. The resulting pComb3X-scFv recombinant phagemids were utilized for the transformation of Escherichia coli XL1-Blue electrocompetent cells via electroporation to facilitate the expression of the phage-displayed scFv fragments, followed by library storage at  $-80^\circ\text{C}$  before selection. The phage display antibody libraries were subjected to panning against TIM-3-His protein using an ELISA assay. Positive clones were distinguished by producing TIM-3 scFv Abs at least five-times higher over the background. These clones were then subcloned for further DNA sequencing investigation.

### 2.3. Construction and expression of whole IgG

The  $V_H$  and  $V_L$ -coding sequences of the mouse anti-TIM-3 Abs were identified through DNA sequencing. The  $V_H$  and  $V_L$  genes were inserted into pCMV3 vectors containing the constant regions of mouse IgG1 light and heavy chains, resulting in the generation of pCMV3-H and pCMV3-L vectors, respectively. The transient expression of whole mouse IgG antibodies was achieved in human embryonic kidney 293 cells through co-transfection with the corresponding pCMV3-H and pCMV3-L vectors for a duration of 6–7 days.

The culture supernatants were then harvested and the Abs were purified using Protein A.

#### 2.4. ELISAs

The specificities and sensitivities of anti-TIM-3 mAbs were assessed using indirect ELISAs. Microplate wells were coated with recombinant proteins overnight at 4 °C, including human TIM-3-His (hTIM-3; Sino Biological, Beijing, China; 10390-H08H), CD137-His (hCD137; Sino Biological, 10041-H08H), OX40-His (hOX40; Sino Biological, 10481-H08H), PD-L1-His (hPD-L1; Sino Biological, 10084-H08H), mouse TIM-3-His (mTIM-3; Sino Biological, 51152-M08H), or cynomolgus TIM-3-hFc (cynTIM-3; Sino Biological, 90312-C02H) at a concentration of 1 µg/mL. Alternatively, the wells were coated with serial dilutions of hTIM-3 or cynTIM-3 protein ranging from 1 µg/mL to 1 pg/mL. The plates were blocked with 5% skimmed milk and then incubated with each anti-TIM-3 mAb or biotin labeled Abs at a concentration of 1 µg/mL for 2 h at 37 °C. After washing, the plates were incubated with horseradish peroxidase (HRP)-conjugated goat anti-mouse IgG (H + L) Ab (ZSGB-BIO, Beijing, China) or streptavidin-HRP at a diluting of 1:5000 for 1 h at 37 °C. A final incubation with TMB substrate solution for 30 min at 37 °C was employed to detect Ab-antigen interaction. The optical density at 450 nm (OD<sub>450</sub>) was measured subsequent to the addition of stop solution. The anti-TIM-3 mAb F38-2E2 served as a positive control.

Sandwich ELISAs were performed to identify distinct binding epitopes of the Abs and quantify the sensitivities of the paired Abs. Capture antibodies were coated at a concentration of 1 µg/mL. The hTIM-3 protein was diluted to a concentration of 1 µg/mL or subjected to serial 10-fold dilutions ranging from 1 µg/mL to 1 pg/mL. The concentration of detection antibodies labeled with biotin was adjusted to 1 µg/mL. All other steps were carried out as previously described.

#### 2.5. SDS-PAGE and western blotting

The purified TIM-3 Abs and hTIM-3 protein were individually mixed with loading buffer with or without 2-mercaptoethanol, and subjected to either boiling for 5 min or left unboiled. Subsequently, they were separated by 10% SDS-PAGE, followed by Coomassie brilliant blue staining and transfer of the proteins onto nitrocellulose membranes. The membranes were blocked with 5% milk in phosphate buffered saline (PBS) for 2 h. TIM-3-specific mAbs were used as the primary Ab at a concentration of 1 µg/mL for 2 h, followed by incubation with goat anti-mouse IgG-HRP (diluted 1:5000) as the secondary Ab for 1 h. Chemiluminescent substrate for HRP was used to visualize the protein bands.

#### 2.6. Flow cytometry

RPMI8226 cells expressing endogenous TIM-3 were collected and subsequently washed with staining buffer containing 1% FBS in PBS. The cell pellets were then resuspended in 100 µl of staining buffer, followed by separate application of each TIM-3 mAb at a concentration of 1 µg/mL for 30 min at room temperature (RT). After washing, the TIM-3 mAbs were identified using an AF647-labeled goat polyclonal secondary Ab specific for mouse IgG (H&L) (Abcam) for 30 min in a dark environment at RT. Finally, the samples were washed, precipitated, and subsequently resuspended in 200 µl of staining buffer. Flow cytometry analysis was performed using a BD LSRFortessa™ flow cytometer.

#### 2.7. Epitope identification and affinity determination using the fortebio octet system

The TIM-3-hFc recombinant protein (Sino Biological, 10390-H02H) was dissolved in saline at a concentration of 5 µg/mL and loaded into each well of an Octet 96-well microplate. Subsequently, it was immobilized onto anti-human IgG Fc capture (AHC) sensors. The tested mouse anti-TIM-3 mAb and all TIM-3 Abs were successively associated onto the protein in the sensors. The ForteBio Octet (ForteBio Inc., CA, USA) assay protocol was conducted as follows: a 60-s baseline (baseline 1), loading of TIM-3-hFc at a concentration of 5 µg/mL for 100 s, another baseline period of 120 s (baseline 2), association of the tested TIM-3 Ab at 5 µg/mL for 300 s to achieve saturation (association 1), and association of all TIM-3 Abs at 5 µg/mL for 180 s (association 2).

The affinities of mouse mAbs for human TIM-3 were determined by employing five serial two-fold dilutions of each mouse anti-TIM-3 mAb along with a negative control (saline) in every experiment. The Octet assay protocol was performed as follows: a baseline of 60 s (baseline 1) was established, followed by loading either 5 µg/mL human TIM-3-hFc or cynTIM-3-hFc for 100 s, another baseline of 120 s (baseline 2), association of the test mAb for 180 s, and followed by disassociation for 300 s. The highest concentration of mAb used was set at 250 nM.

#### 2.8. Gal-9 binding to TIM-3 and the effect of TIM-3 mAbs on the interaction between Gal-9 and TIM-3

The binding of Gal-9 to TIM-3 was initially assessed. Recombinant human Gal-9 (R&D Systems, 3535-GA) was diluted to a concentration of 1 µg/mL and immobilized on ELISA plates overnight at 4 °C. The plates were washed with PBS and subsequently blocked with 2% bovine serum albumin (BSA) in PBS. Then, human TIM-3-His protein (Sino Biological) was applied at a concentration of 1 µg/mL in 0.5% BSA/PBS for 2 h at 37 °C. After the washing step, the plates were incubated with an HRP-conjugated mouse anti-His mAb (Abmart, Shanghai, China) at 37 °C for 1 h. Subsequently, the plates were washed and detection was performed using TMB reagent. OD<sub>450</sub> was measured on a Bio-Tek plate reader after addition of stop solution.

A Gal9/TIM-3 complex was formed via the reaction of Gal-9 with TIM-3-His protein on a plate, in order to ascertain whether our

anti-TIM-3 mAbs and Gal-9 bind to similar epitopes on TIM-3. This complex was detected by applying 1 µg/mL of each TIM-3 mAb for 2 h at 37 °C after washing. The TIM-3 mAbs were detected using an HRP-coupled goat anti-mouse IgG (H + L) Ab (ZSGB-BIO, Beijing, China), followed by washing and detection with reagents. Once the stop solution was added, the OD<sub>450</sub> was measured.

The Gal-9 was initially immobilized on a plate, followed by incubation with 5 µg/mL of TIM-3-His protein and either 10 µg/mL or 50 µg/mL anti-TIM-3 mAbs at 37 °C for 2 h to evaluate the inhibitory effect of the mAbs on the interaction between Gal-9 and TIM-3. Subsequently, after washing, the formation of the Gal-9/TIM-3 complex was identified using anti-His-HRP Abs, while the presence of the Gal-9/TIM-3/anti-TIM-3 complex was identified by anti-Ms-HRP Abs.

2.9. Measurement of CEACAM-1/TIM-3 and HMGB-1/TIM-3 complex reactivity with TIM-3-specific mAbs

We further investigated the reactivity of our TIM-3 antibodies with the CEACAM-1/TIM-3 and HMGB-1/TIM-3 complexes. Recombinant proteins, including CEACAM-1-His (Sino Biological, 10822-H08H) and HMGB-1-His (Sino Biological, 10326-H08H), were immobilized on ELISA plates at a concentration of 1 µg/mL and incubated overnight at 4 °C. The plates were washed with PBS and then blocked with 2% BSA in PBS. Subsequently, TIM-3-His protein at a concentration of 1 µg/mL in 0.5% BSA/PBS was applied for a duration of 2 h at 37 °C. After washing, each anti-TIM-3 mAb was applied at 1 µg/mL for 2 h at 37 °C to detect complexes formed by CAECAM1/TIM-3 or HMGB-1/TIM-3. The TIM-3 mAbs were identified by an HRP-coupled goat anti-mouse IgG (H + L) Ab, followed by washing and detection with TMB reagents. OD<sub>450</sub> was measured after the addition of a stop solution.

2.10. Statistical analysis

Statistical analysis was performed using GraphPad Prism 10 software. Specifically, the analysis included a Mann–Whitney test, Analysis of Variance with post-hot multiple comparisons, and multiple unpaired t-tests. Differences were considered significant when p < 0.05. Cut-off values in ELISA were calculated from 2.1 times of the mean absorbance of negative control or blank control.

3. Results

3.1. Sequence analyses of mouse anti-human TIM-3 monoclonal antibodies

We isolated four clones, designated as MsT001, MsT065, MsT229, and MsT286, from the scFv phage display library derived from an immunized mouse that exhibited strong reactivity to hTIM-3 in ELISAs. By employing the ABodyBuilder software (<http://opig.stats.ox.ac.uk/webapps/newsabdab/sabpred/abodybuilder/>) with Kabat modeling for amino acid sequence analysis of these phage clones, we accurately identified three complementarity-determining regions (CDRs) within both V<sub>H</sub> and V<sub>L</sub> chains for each mAb (Fig. 1). Our findings revealed that MsT001 and MsT065 shared identical V<sub>H</sub>-CDR3 sequences. In contrast, the V<sub>H</sub>-CDR3 sequences of MsT229 and MsT286 displayed significant divergence compared to those of MsT001 and MsT065, with nine amino acid variations.

3.2. Specificities of the anti-TIM-3 antibodies

In subsequent investigations, anti-TIM-3 IgG mAbs with purities of >95% (Fig. 2A) were used. The specificities of these TIM-3 mAbs were confirmed through western blotting, ELISAs, and flow cytometry. Anti-TIM-3 mAb F38-2E2 was employed as a positive control. TIM-3 mAbs F38-2E2, MsT229, and MsT286 mainly reacted with non-denatured TIM-3 protein, but they did not react with denatured TIM3 protein, according to western blot analysis (Fig. 2B), suggesting that they were able to recognize conformational epitopes of TIM-3 protein. The detection of both native and denatured TIM-3 proteins by MsT001 and MsT065 (Fig. 2B) suggested that they were able to identify linear epitopes of the TIM-3 protein.

V <sub>H</sub>	FR1	CDR1	FR2	CDR2	FR3	CDR3	FR4
	1	3031 3536	49 50	6667		9899 109110	120
MsT001-V <sub>H</sub> :	EVQLQQSGAEVMPGASVKMSCKTSGYTFDYL	IHWVKRPGQLVWIG	AI	DTSDSYASYNQKFKGKATL	TLDESSRTAYMQLSSLTSEDSAVYFCTG	-----EGLD	YWGQGTSTVSS 114
MsT065-V <sub>H</sub> :	QVQLIQSGAELVMPGASVKMSCKASGYTFDHL	MHWVKRPGQLVWIG	AI	DTSDSYASYNRKF	GKATLTVDESSRTAYMQLSSLTSEDSAVVY	CAG-----EGLD	YWGQGTSTVSS 114
MsT229-V <sub>H</sub> :	EIQLVQSGPELVKPGASMKMSCKASGYSTFT	GMNHWVKRPGQLVWIG	AI	INPQTGGTSYNQFRGKATL	TVDKSSNTAYMELL	SLTSEDSAVVYCARERGFDS	PGFPYWGQGLTVTVA 120
MsT286-V <sub>H</sub> :	QVQLQQSGPELVKPGASMKMSCKASGYSTFT	GMNHWVKRPGQLVWIG	AI	INPQTGGTSYNQFRGKATL	TVDKSSNTAYMELL	SLTSEDSAVVYCARERGFDS	PGFPYWGQGLTVTVA 120
V <sub>L</sub>	FR1	CDR1	FR2	CDR2	FR3	CDR3	FR4
	1	2324	3940	5455 6162		9394 103104	113
MsT001-V <sub>L</sub> :	DIQMTQTPPLSLPVSLGDAQISCRSSQSLVHS	NGNTYLNWY	LQKPGQSPKLLIYK	VSRFSGVPDRFSGSGSGTDFTL	TKSRVEAE	DLGVYFCSQSTHVPPL	TFGAGTKLELK 113
MsT065-V <sub>L</sub> :	DVVMQTTPPLSLPVSLGDAQISCRSSQNLVHS	NGNTYLNWY	LQKPGQSPKLLIYK	VSNRFS	GVDRFSGSGSGTDFTL	TKSRVEAE	DLGVYFCSQSTHVP-PLTFGAGTKLEMK 112
MsT229-V <sub>L</sub> :	DIQMTQTSSLSASLGDRVITISCRASQDI	-----SNYLNWY	QKPGDGT	VKLLIYYSRLHS	GVPSRFSGSGSGTDYSLTISNLE	QEDIATYFCQQGNT-LPLTFGAGTKLELK 107	
MsT286-V <sub>L</sub> :	DIVLTQSPASLAVSLGQRATISCKASQSV-DYD	GDSYMNWY	QKPGQPPKLLIYAASNL	ESGIPARFSGSGSGTDFTLN	IHPVEE	EAAATYYCQSQSNE-DPYTFGGG	TKLEIK 111

Fig. 1. Alignment of the V<sub>H</sub> and V<sub>L</sub> amino acid sequences in TIM-3 antibodies. The framework regions (FRs) and complementarity-determining regions (CDRs) within the V<sub>H</sub> and V<sub>L</sub> regions were highlighted accordingly. The absence of no amino acid at a certain location is indicated by the symbol "-".

Our TIM-3 mAbs interacted with the hTIM-3 protein; they were inactive against hCD137, hPD-L1, and hOX40. In the ELISAs, MsT229 and MsT286 displayed a cross-reactivity with cynTIM-3, and MsT286 showed a slight cross-reactivity with mTIM-3, indicating that these two mAbs may not precisely identify the same locations on TIM-3 (Fig. 2C). The anti-TIM-3 mAbs exhibited reactivity towards both exogenous and endogenous surface TIM-3 protein on 293FT cells expressing TIM-3 (data not shown), as well as on the

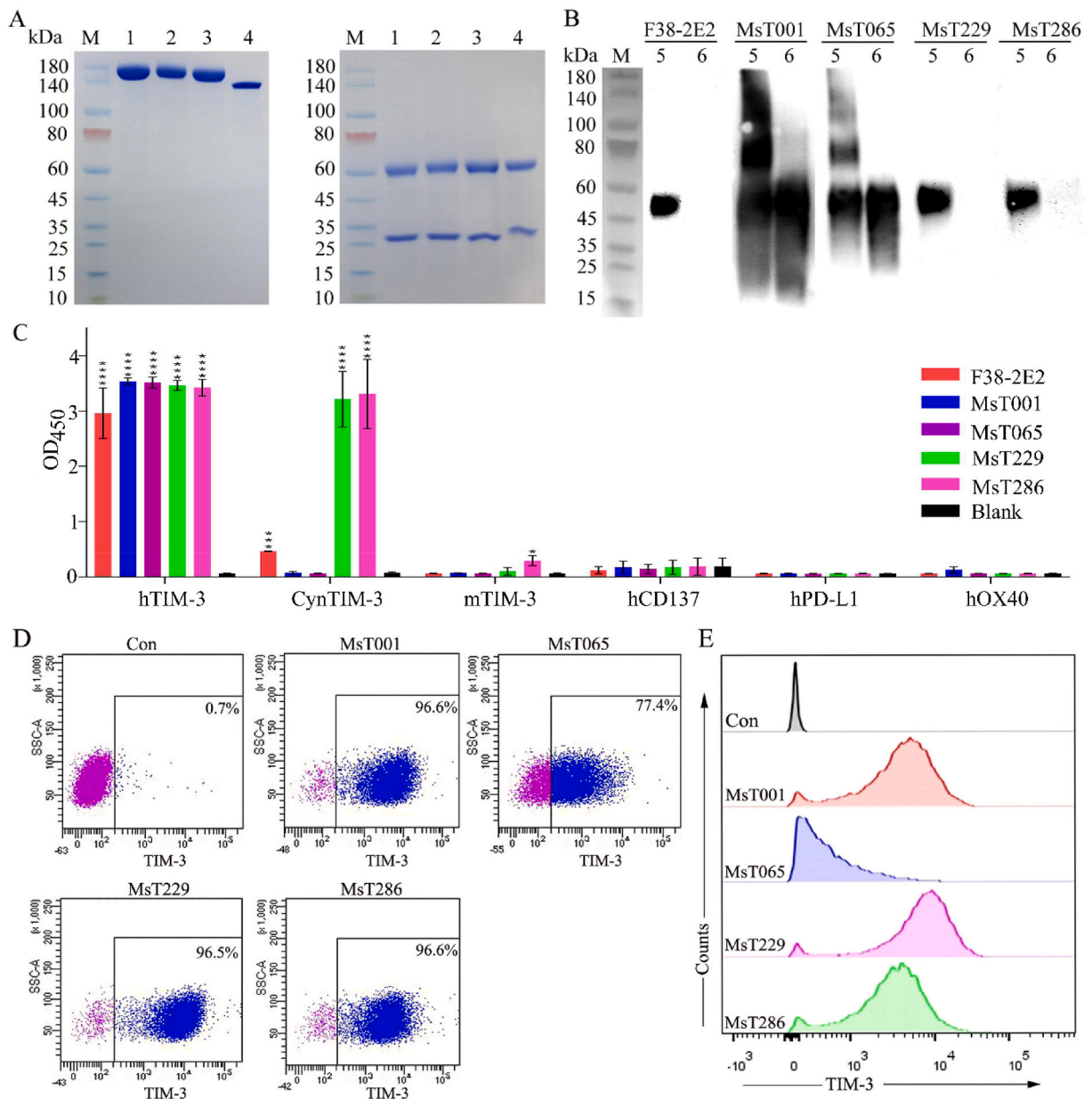


**Fig. 2.** Analysis of the specificities of TIM-3 antibodies. (A) The purified TIM-3-specific mouse IgG antibodies (Abs) were subjected to SDS-PAGE analysis under non-denaturing (left panel) and denaturing (right panel) conditions. The separate images were cropped from the same gel. The entire image of the gel is shown in [Supplementary Figure S1](#) (B) The recognition characteristics of TIM-3 Abs for native and denatured TIM-3 protein in western blot analysis. The combined images were cropped from different images. The entire image of western blots is shown in [Supplementary Figure S2](#) (C) The specificity of the anti-TIM-3 mAbs was assessed by ELISAs. The columns represent mean  $\pm$  standard deviation (SD) of triplicates. Statistical significance was indicated as \*\*\*\*p < 0.0001, \*\*\*p < 0.001, and \*p < 0.05 compared with Blank. Consistent results were observed in three independent experiments. (D, E) Reactivities of anti-TIM-3 mAbs towards endogenous cell surface TIM-3 protein on the RPMI8226 multiple myeloma cell line were assessed using flow cytometry. The RPMI8226 cells without addition of TIM-3 mAb were used as control (Con). Representative dot plots (D) and histograms (E) depicting the TIM-3 expression by flow cytometry were generated. M: molecular weight marker; 1 = MsT001; 2 = MsT065; 3 = MsT229; 4 = MsT286; 5 = non-denatured TIM-3 protein; 6 = denatured TIM-3 protein; hTIM-3 = human TIM-3; cynTIM-3 = cynomolgus TIM-3; mTIM-3 = mouse TIM-3; hCD137 = human CD137; hPD-L1 = human PD-L1; hOX40 = human OX40.

multiple myeloma cell line PRMI8226, as determined by flow cytometry (Fig. 2D and E). These findings showed that our TIM-3 mAbs could recognize both linear and conformational epitopes of TIM-3 with excellent specificities.

### 3.3. Epitope-binding characteristics of the anti-TIM-3 antibodies

The epitope-binding characteristics of the TIM-3 Abs were assessed using sandwich ELISAs and the ForteBio Octet system. The results demonstrated that MsT001 and MsT065 did not impede the binding of MsT229 and MsT286, thereby confirming their recognition of distinct epitopes on TIM-3 (Fig. 3A and B). The binding of MsT001 to TIM-3 was found to impede the interaction with MsT065, while the binding of MsT065 to TIM-3 did not hinder the binding of MsT001. This observation suggests that these two antibodies recognize partially overlapped epitopes on TIM-3. The simultaneously binding of MsT001 and MsT001-Bio to TIM-3 was observed in the sandwich ELISA (Fig. 3A), indicating the presence of at least two separate binding sites for MsT001 on TIM-3, which can be identified using the same Ab in a sandwich ELISA. The binding of MsT229, MsT286, or F38-2E2 (data not shown) to TIM-3 mutually impeded the interaction between each other and TIM-3 (Fig. 3B). The recognition of conformational epitopes on the TIM-3 protein led to speculate that the binding of MsT229, MsT286, or F38-2E2 may induce a conformational shift in TIM-3, thereby interfering with their mutual interaction.

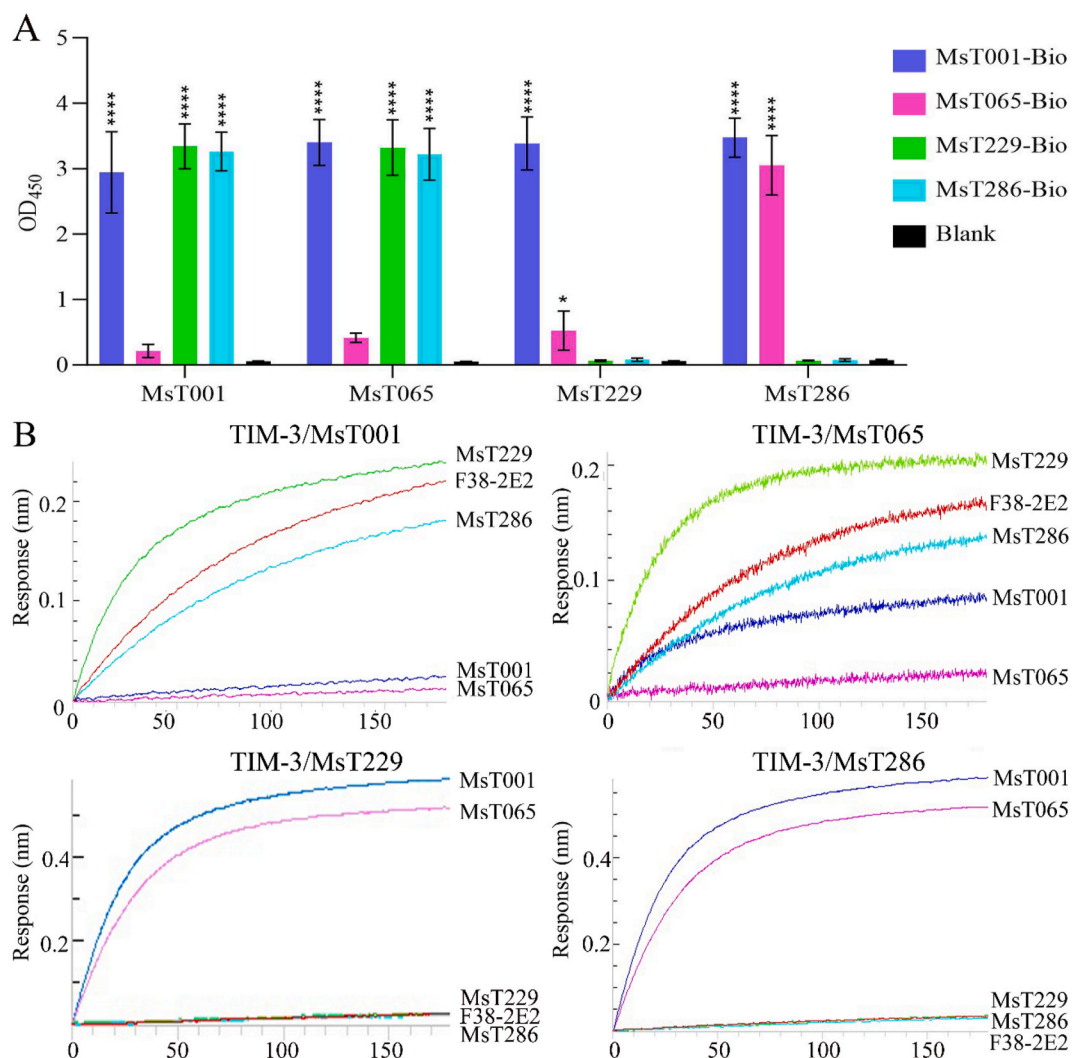


**Fig. 3.** Binding characteristics of TIM-3-specific antibodies. (A) Identification of distinct epitopes of TIM-3 through sandwich ELISAs. (B) The verification of various epitopes on TIM-3 using the ForteBio Octet system. A sensorgram shows TIM-3-Fc on the anti-human IgG Fc capture sensors, which has been linked to an anti-TIM-3 antibody to achieve saturation, and then bind to all TIM-3 antibodies. Statistical significance was indicated as \*\*\* $p < 0.0001$  and \* $p < 0.05$  compared with Blank.

### 3.4. Sensitivities of the anti-TIM-3 antibodies

MsT001 and MsT286 demonstrated similar sensitivities of 1 ng/mL to the TIM-3-His recombinant protein, while MsT065 and MsT229 showed a sensitivity of 10 ng/mL. The commercial antibody F38-2E2 had a sensitivity of 100 ng/mL (Fig. 4A, left). The sensitivities of MsT001-Bio (100 pg/mL), MsT286-Bio (100 pg/mL), and MsT229-Bio (1 ng/mL) were ten times higher than the corresponding unlabeled mAbs, whereas the sensitivity of MsT065-Bio remained unchanged (Fig. 4A, right). When using MsT001 as a capture Ab and either MsT229-Bio or MsT286-Bio as detecting Abs, the sandwich ELISA demonstrated the highest sensitivities of 10 pg/mL for TIM-3 (Fig. 4B and Table 1).

### 3.5. Affinities of the anti-TIM-3 antibodies

The affinities of the TIM-3 mAbs were determined using the ForteBio Octet system (Fig. 5). The  $K_D$  values for F38-2E2, MsT001, MsT065, MsT229, and MsT286 binding to TIM-3 were  $8.40 \times 10^{-10}$  M,  $4.61 \times 10^{-11}$  M,  $1.59 \times 10^{-9}$  M,  $3.70 \times 10^{-9}$  M, and  $7.73 \times$

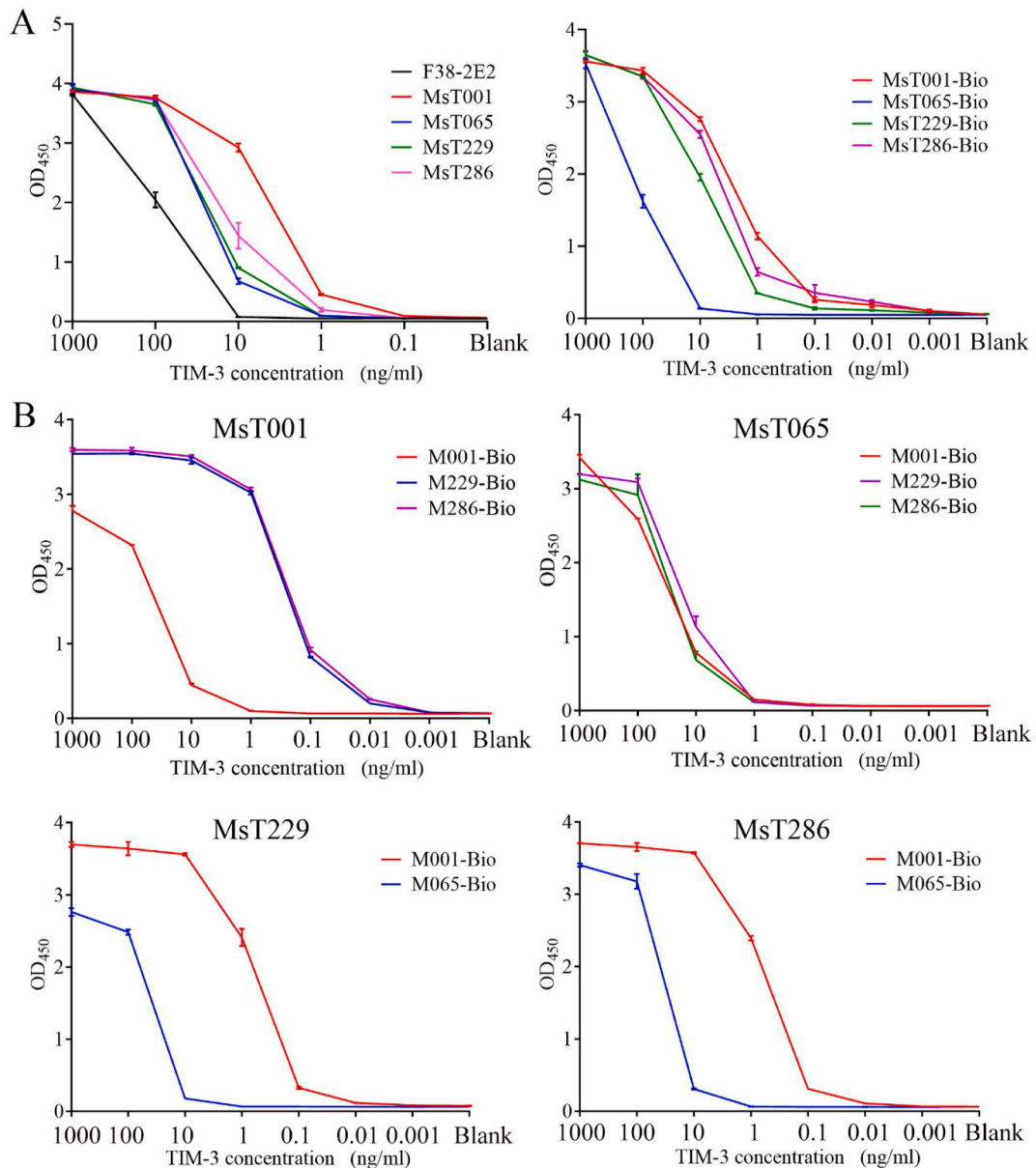


**Fig. 4.** Sensitivities of TIM-3-specific antibodies. (A) Sensitivities of unlabeled (left) and biotin-labeled (right) TIM-3 monoclonal antibodies were determined by indirect ELISAs. (B) The sensitivities of anti-TIM-3 antibody pairs in sandwich ELISA assays.

$10^{-10}$  M, respectively. Their corresponding  $R^2$  values were 0.9956, 0.9929, 0.9917, 0.9702, and 0.9965.

### 3.6. Characteristics of the anti-TIM-3 antibodies in detecting cynomolgus TIM-3

According to the results shown in Fig. 2C, it has been observed that both MsT229 and MsT286 exhibit reactivity toward cynTIM-3. Subsequently, the sensitivities and affinities of these two Abs to cynTIM-3 were further determined. Sensitivities to cynTIM-3 were 1 ng/mL and 100 pg/mL for unlabeled and biotin-labeled MsT229 and MsT286 (Fig. 6A), respectively, as measured by ELISA. The  $K_D$  values for the binding of MsT229 and MsT286 to cynTIM-3 were determined to be  $1.79 \times 10^{-11}$  M and  $9.14 \times 10^{-10}$  M, respectively, with corresponding  $R^2$  values of 0.9899 and 0.9932 (Fig. 6B).

### 3.7. An analysis comparing the binding characteristics of the anti-TIM-3 Abs and its ligands on TIM-3

The reported ligands for TIM-3 include Gal-9, PtdSer, HMGB-1 and CEACAM-1, which bind to different regions on the extracellular IgV domain of TIM-3. Specifically, the binding sites for CEACAM-1, HMGB-1, and PtdSer are located in FG and/or CC' loops [13,19,33,34], while the Gal-9-binding site is predicted to be N-linked sugars on the opposite side of the FGCC' face of TIM-3 [17]. In this study, we firstly bound hTIM-3-His onto a Gal-9 protein-coated ELISA plate and then detected the formation of the Gal9/TIM-3 complex using an anti-His Ab (Fig. 7A). We subsequently employed anti-TIM-3 Abs to detect TIM-3 protein captured by Gal-9 and observed that MsT001 and MsT065 identified the Gal-9/TIM-3 complex in the ELISA assay (Fig. 7B), indicating their binding to distinct epitopes on TIM-3 compared to Gal-9. MsT229, MsT286, and F38-2E2, on the other hand, were unable to recognize the Gal-9/TIM-3 complex (Fig. 7B).

Furthermore, our finding demonstrated that MsT001 and MsT065 are capable of detecting CEACAM-1/TIM-3 and HMGB-1/TIM-3 complexes, whereas MsT229 and MsT286 exhibit no such capability (Fig. 7C and D). We have observed that MsT229, MsT286, and F38-2E2 recognized conformational epitopes of TIM-3 (Fig. 2B). Consequently, we hypothesize that the binding of Gal-9, HMGB-1 or CEACAM-1 may induce a conformational alter in TIM-3, thereby interfering with the binding of TIM-3 Abs.

We subsequently investigated whether the presence of TIM-3 antibodies affected the binding of Gal-9 to TIM-3. The results showed that the interaction between TIM-3 and Gal-9 were inhibited upon increasing concentration of MsT229 and MsT286 (Fig. 8). The Gal-9 protein was found to interact with the TIM-3/MsT001 complex, while it did not exhibit any interaction with TIM-3/MsT229 or TIM-3/MsT286 complexes (Fig. 8). These findings suggested that the binding of MsT229 or MsT286 to TIM-3 could hinder the binding of Gal-9 to TIM-3.

## 4. Discussion

We have successfully produced unique mouse anti-human TIM-3 mAbs in this investigation. Specifically, the  $V_H$ -CDR3 regions of MsT001 and MsT065 share identical sequences, so do the  $V_H$ -CDR3 regions between MsT229 and MsT286. However, there is a significant divergence in the  $V_H$ -CDR3 region when comparing MsT001/MsT065 to MsT229/MsT286. The performances of these Abs were in line with the results of the sequence analysis, which enabled them to recognize distinct epitopes on TIM-3. MsT001 and MsT065 were able to identify linear epitopes on TIM-3, while MsT229, MsT289, and the commercial TIM-3 functional Ab F38-2E2 recognized conformational epitopes on TIM-3. Our TIM-3 Abs showed high specificity towards TIM-3. MsT001 and MsT065 only reacted with human TIM-3. MsT229 and MsT286 exhibited reactivity to cynomolgus TIM-3, while MsT286 showed a weak response to mouse TIM-3. The homology of TIM-3 between human and cynomolgus monkeys is approximately 85%; therefore, it is likely that the binding sites of MsT229 and MsT286 are located in the highly conserved region of TIM-3 between these two species.

The expression of TIM-3 has also been observed on tumor cells. In the context of hematological malignancies, TIM-3 expression has been documented in multiple myeloma, myelodysplastic syndrome (MDS), and certain types of leukemias [35–37]. TIM-3 serves as a definitive marker to distinguish leukemic stem cells from normal hematopoietic stem cells [37–39]. In MDS and acute myeloid leukemia, TIM-3 blockade results in 50–60% response rates [6,39]. The TIM-3 antibodies we developed demonstrated the ability to detect surface expression of TIM-3 on the RPMI8226 multiple myeloma cell line.

Different epitopes and locations on TIM-3 were recognized by our TIM-3 Abs. Two different antibodies, MsT001 and MsT065, identified partially overlapping epitopes on TIM-3. MsT001 binding to TIM-3 may affect MsT065's binding through steric hindrance. MsT001 may identified at least two separate linear epitopes on TIM-3, which exhibited the optimal sensitivity and affinity towards the protein. Although the determination results of MsT229 and MsT286 showed a high level of consistency, it is worth noting that

**Table 1**  
Sensitivities of anti-TIM-3 antibodies in sandwich ELISAs.

Capture mAbs	Detecting mAbs			
	MsT001-Bio	MsT065-Bio	MsT229-Bio	MsT286-Bio
MsT001	10.0	–	0.01	0.01
MsT065	1.0	–	1.0	1.0
MsT229	0.1	10	–	–
MsT286	0.1	10	–	–

The numbers indicate the detectable concentration of hTIM-3 protein (ng/ml). Similar findings were observed in three independent experiments.

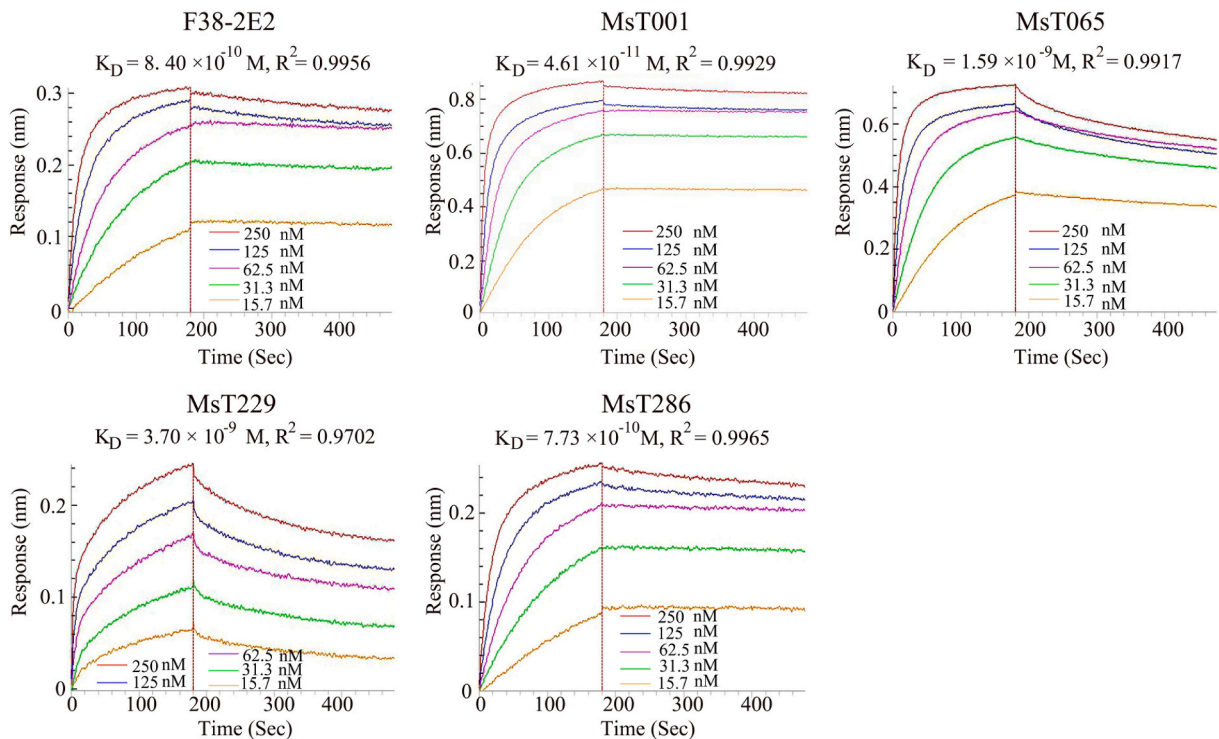


**Fig. 5.** TIM-3 antibodies' affinities for human TIM-3 as assessed by the ForteBio Octet system. The original sensorgram shows TIM-3-Fc on the anti-human IgG Fc capture sensors, which bound to various concentrations of TIM-3 antibodies. The binding affinity parameter  $K_D$  was determined by fitting the sensorgram.  $R^2$  is the coefficient of determination to estimate the goodness of the curve fit as reported by ForteBio Data Analysis Software 9.0.

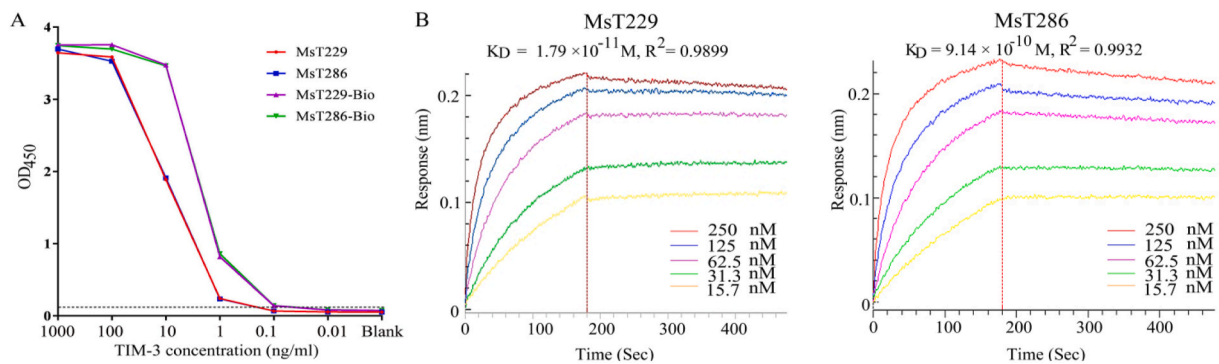


**Fig. 6.** The sensitivities and affinities of TIM-3 antibodies to cynomolgus TIM-3 protein. (A) The sensitivities of the unlabeled and biotin-labeled TIM-3 antibodies were assessed by ELISAs. (B) The affinities of the TIM-3 antibodies for cynTIM-3 were assessed using the ForteBio Octet system.

differences in their binding sites may exist. The finding that MsT286 showed a weak cross-reactivity with mouse TIM-3, while MsT229 demonstrated no such reactivity, provided further support for this argument.

The unique recognition epitopes of our TIM-3 Abs allowed for the detection of soluble TIM-3 (sTIM-3). Metalloproteinases can cleave TIM-3 to produce sTIM-3, or alternative splicing of the TIM-3 gene results in the expression of sTIM-3 [40,41]. Therefore, the concentration of sTIM-3 may serve as a soluble indicator of immune exhaustion and reflect the level of membrane expression of TIM-3 [40]. The use of MsT001 as a capture Ab, along with biotin-labeled MsT229 or MsT286 as detection Abs, demonstrated the highest sensitivity in detecting sTIM-3 (10 pg/mL), surpassing the current ELISA assay (approximately 1 ng/mL). The sensitivities of our TIM-3 Abs have demonstrated a 10–100 times increase compared to that of the commercial TIM-3 antibody F38-2E2, thereby significantly enhancing the potential for clinical detection of TIM-3. Additionally, MsT001 and MsT065 exhibit distinct epitope recognition on TIM-3 in comparison to F38-2E2, thus offering an alternative antibody pairing option for the detection of sTIM-3.

The complete elucidation of the specific ligand-receptor interaction interfered by TIM-3 blocking Abs remains to be determined due

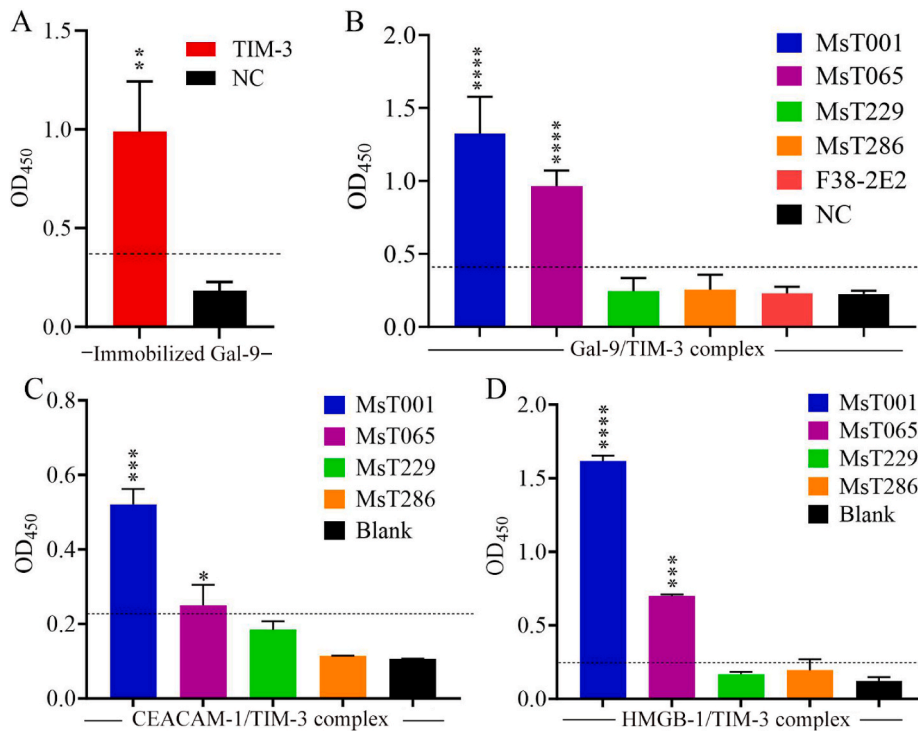


**Fig. 7.** The binding characteristics of anti-TIM-3 antibodies to ligand/TIM-3 complex. The binding of mouse anti-human TIM-3 antibodies to human Gal-9/TIM-3 (B), CEACAM-1/TIM-3 (C) or HMGB-1/TIM-3 complex (D) was detected using anti-mouse antibodies in ELISAs. Prior to being treated with mouse anti-TIM-3 mAbs, TIM-3-His were firstly attached to immobilized Gal-9, CEACAM-1, or HMGB-1 in ELISA plates. Reaction complexes were identified using anti-Ms-(H + L)-HRP. NC = negative control without TIM-3 protein; Blank = blank control without an anti-TIM-3 antibody. Horizontal lines indicate the cut-off, which were determined based on 2.1 times the mean absorbance of the negative control or blank. Statistical significance was indicated as \*\*\*\* $p < 0.0001$ , \*\*\* $p < 0.001$ , \*\* $p < 0.01$ , and \* $p < 0.05$  compared with NC or Blank.

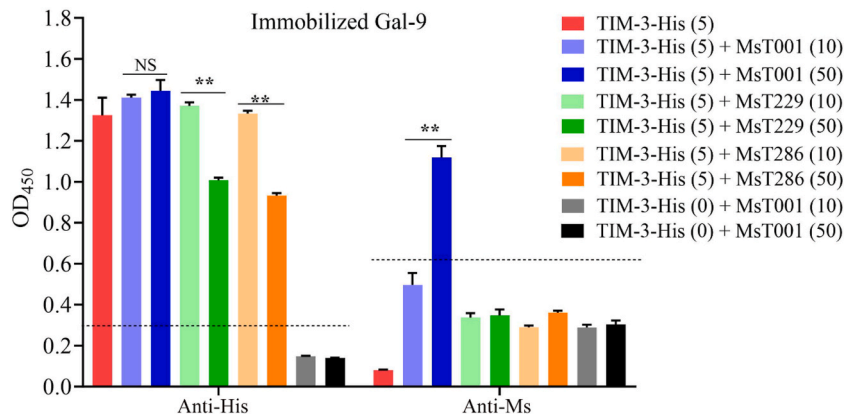


**Fig. 8.** Anti-TIM-3 antibodies inhibited Gal-9 from binding to TIM-3. Binding of hTIM-3-His to plate-bound Gal-9 was evaluated via ELISA in the presence of anti-TIM-3 antibodies. The reaction complex was detected using anti-His-HRP or anti-Ms-(H + L)-HRP. Horizontal lines indicate the cut-off, which were determined based on 2.1 times the mean absorbance of the negative control without TIM-3 protein. Statistical significance was assessed using multiple unpaired t-tests (\*\* $p < 0.01$  compared with negative control). NS indicates no statistically significance.

to the presence of multiple ligands for TIM-3. The binding site of Gal-9 is located opposite to that of CEACAM-1, HMGB-1, and PtdSer on TIM-3 [13,17,19,33,34]. Functionally efficacious anti-murine Tim-3 Abs (RMT3-23, 5D12, and B8.2C12), which bind distinct epitopes, as well as an anti-human TIM-3 Ab (F38-2E2), disrupt the binding to both PtdSer and CEACAM-1 [34]. The compound RMT3-23 was found to effectively inhibit the interaction between TIM-3 and Gal-9 [42], as well as suppress the dose-dependent TNF- $\alpha$  production induced by Gal-9 in cultured DCs [43]. The function effects of 5D12 and B8.2C12 have been reported to be exerted presumably through allosteric inhibition [13,15]. Meanwhile, 2E2 has the ability to inhibit Gal-9-mediated TNF- $\alpha$  secretion from human

monocytes [11,42]. The fully human anti-TIM-3 mAb, M6903, shares overlapping epitopes with F38-2E2 and effectively inhibits the binding of TIM-3 to PtdSer, CEACAM-1, and Gal-9 [16]. The humanized mAb Sabatolimab has been demonstrated to effectively inhibit the interaction between TIM-3 and its ligands PtdSer/Gal-9 [44]. Additionally, it remains unclear whether Tim-3 can simultaneously bind to its ligands, including CEACAM-1 and PtdSer [34].

Our data demonstrated that the interaction between Gal-9, CEACAM-1, or HMGB-1 and TIM-3 hindered the binding of MsT229 and MsT286, while it had no impact on the binding of MsT001 and MsT065. Additionally, further study is required to fully understand the binding characteristics associated with the interaction between TIM-3 and these TIM-3 mAbs/Ptdser. Our findings indicated that both MsT001 and MsT065 possess the capability to bind TIM-3 monomers and TIM-3 within a complex, regardless of whether its ligand undergoes mutation [45] or if TIM-3 is bound to its ligand. This facilitates the identification of TIM-3 expression in the microenvironment of human organism. However, MsT229, MsT286, and commercial TIM-3 antibodies F38-2E2 do not demonstrate this binding ability.

MsT229 and MsT286 exhibited a dose-dependent inhibition of the interaction between Gal-9 and TIM-3. Importantly, both MsT229 and MsT286 specifically targeted a conformational epitope on TIM-3. The conformational epitopes of a protein are formed by several separate regions in its sequence, which subsequently become spatially juxtaposed through the process of protein folding. The binding of a ligand or Ab may induce a conformational alteration in the antigen's structure, leading to allosteric inhibition and potential interference with the binding of other substances at distinct protein sites. The specific conformational details of human TIM-3 have remained elusive to date, hindering a comprehensive understanding of these ligand interactions [38]. Based on our findings and other published reports, it is hypothesized that the binding sites of Gal-9, CEACAM-1, HMGB-1, MsT229, and MsT286 may be closely linked to a conformational epitope of TIM-3. Additional experimental validation is warranted to confirm this hypothesis.

In conclusion, we have successfully developed novel anti-human TIM-3 mAbs that exhibit high sensitivity and affinity for the TIM-3 protein. These Abs are capable of detecting membrane and sTIM-3 proteins because they recognize both linear and conformational epitopes on TIM-3. Importantly, our TIM-3 Abs may cause a conformational shift in TIM-3 that prevents ligands from binding to TIM-3. The study has some limitations that should be considered, including the *in vitro* and *in vivo* functionality of TIM-3 Abs. Our subsequent investigation will also explore and evaluate the efficacy of these anti-TIM-3 antibodies both as monotherapy and in combination with other immune checkpoint inhibitors. Generally, this study's preliminary findings offer valuable insights for understanding and targeting human TIM-3.

#### Ethics statement

This study involving mice was reviewed and approved by the Animal Experimental Ethics Committee of Beijing Chest Hospital, Capital Medical University (NO. 2020-012). The animal research adheres to the ARRIVE guidelines.

#### Data availability statement

The authors confirm that the data supporting the findings of this study are available within the article.

#### CRedit authorship contribution statement

**Zhuohong Yan:** Writing – review & editing, Writing – original draft, Visualization, Validation, Software, Project administration, Methodology, Investigation, Funding acquisition, Formal analysis, Data curation. **Teng Ma:** Writing – review & editing, Writing – original draft, Investigation. **Xiaojue Wang:** Software, Methodology, Investigation, Data curation. **Ling Yi:** Resources, Investigation, Formal analysis. **Panjian Wei:** Investigation. **Hongtao Zhang:** Resources, Funding acquisition. **Jinghui Wang:** Writing – review & editing, Writing – original draft, Resources, Funding acquisition.

#### Declaration of competing interest

The authors declare that they have no known competing financial interests or personal relationships that could have appeared to influence the work reported in this paper.

#### Acknowledgments

This study was supported by the grants from the Beijing Municipal Administration of Hospitals Incubating Program (PX2020065), the Capital Medical University Research and Cultivation Fund (PYZ22135), and the Beijing Tongzhou District Science and Technology Plan Project (KJ2023CX049).

#### Appendix A. Supplementary data

Supplementary data to this article can be found online at <https://doi.org/10.1016/j.heliyon.2024.e28126>.

## References

- [1] X. Chu, et al., Co-Inhibition of TIGIT and PD-1/PD-L1 in cancer immunotherapy: mechanisms and clinical trials, *Mol. Cancer* 22 (1) (2023) 93.
- [2] T. Zhang, et al., Genetic characteristics involving the PD-1/PD-L1/L2 and CD73/A2aR axes and the immunosuppressive microenvironment in DLBCL, *J Immunother Cancer* 10 (4) (2022).
- [3] M. Nie, et al., The dual role of CD70 in B-cell lymphomagenesis, *Clin. Transl. Med.* 12 (12) (2022) e1118.
- [4] Y. Lu, et al., OX40 shapes an inflamed tumor immune microenvironment and predicts response to immunochemotherapy in diffuse large B-cell lymphoma, *Clin. Immunol.* 251 (2023) 109637.
- [5] Y. Wolf, A.C. Anderson, V.K. Kuchroo, TIM3 comes of age as an inhibitory receptor, *Nat. Rev. Immunol.* 20 (3) (2020) 173–185.
- [6] K.O. Dixon, et al., TIM-3 restrains anti-tumour immunity by regulating inflammasome activation, *Nature* 595 (7865) (2021) 101–106.
- [7] L. Cai, et al., Targeting LAG-3, TIM-3, and TIGIT for cancer immunotherapy, *J. Hematol. Oncol.* 16 (1) (2023) 101.
- [8] O. Pagliano, et al., Tim-3 mediates T cell trogocytosis to limit antitumor immunity, *J. Clin. Invest.* 132 (9) (2022).
- [9] N. Acharya, C. Sabatos-Peyton, A.C. Anderson, Tim-3 finds its place in the cancer immunotherapy landscape, *J Immunother Cancer* 8 (1) (2020).
- [10] L. Monney, et al., Th1-specific cell surface protein Tim-3 regulates macrophage activation and severity of an autoimmune disease, *Nature* 415 (6871) (2002) 536–541.
- [11] W.D. Hastings, et al., TIM-3 is expressed on activated human CD4+ T cells and regulates Th1 and Th17 cytokines, *Eur. J. Immunol.* 39 (9) (2009) 2492–2501.
- [12] K. Sakuishi, et al., TIM3(+)/FOXP3(+) regulatory T cells are tissue-specific promoters of T-cell dysfunction in cancer, *OncoImmunology* 2 (4) (2013) e23849.
- [13] S. Chiba, et al., Tumor-infiltrating DCs suppress nucleic acid-mediated innate immune responses through interactions between the receptor TIM-3 and the alarmin HMGB1, *Nat. Immunol.* 13 (9) (2012) 832–842.
- [14] L.C. Ndhlovu, et al., Tim-3 marks human natural killer cell maturation and suppresses cell-mediated cytotoxicity, *Blood* 119 (16) (2012) 3734–3743.
- [15] M. Das, C. Zhu, V.K. Kuchroo, Tim-3 and its role in regulating anti-tumor immunity, *Immunol. Rev.* 276 (1) (2017) 97–111.
- [16] D. Zhang, et al., Identification and characterization of M6903, an antagonistic anti-TIM-3 monoclonal antibody, *OncoImmunology* 9 (1) (2020) 1744921.
- [17] C. Zhu, et al., The Tim-3 ligand galectin-9 negatively regulates T helper type 1 immunity, *Nat. Immunol.* 6 (12) (2005) 1245–1252.
- [18] M. Nakayama, et al., Tim-3 mediates phagocytosis of apoptotic cells and cross-presentation, *Blood* 113 (16) (2009) 3821–3830.
- [19] Y.H. Huang, et al., CEACAM1 regulates TIM-3-mediated tolerance and exhaustion, *Nature* 517 (7534) (2015) 386–390.
- [20] H. Li, et al., Tim-3/galectin-9 signaling pathway mediates T-cell dysfunction and predicts poor prognosis in patients with hepatitis B virus-associated hepatocellular carcinoma, *Hepatology* 56 (4) (2012) 1342–1351.
- [21] M. Roussel, et al., Functional characterization of PD1+TIM3+ tumor-infiltrating T cells in DLBCL and effects of PD1 or TIM3 blockade, *Blood Adv* 5 (7) (2021) 1816–1829.
- [22] C. Granier, et al., Tim-3 expression on tumor-infiltrating PD-1(+)/CD8(-) T cells correlates with poor clinical outcome in renal cell carcinoma, *Cancer Res.* 77 (5) (2017) 1075–1082.
- [23] J. Fucikova, et al., TIM-3 dictates functional orientation of the immune infiltrate in ovarian cancer, *Clin. Cancer Res.* 25 (15) (2019) 4820–4831.
- [24] M. Klapholz, et al., Presence of Tim3(+) and PD-1(+) CD8(+) T cells identifies microsatellite stable colorectal carcinomas with immune exhaustion and distinct clinicopathological features, *J. Pathol.* 257 (2) (2022) 186–197.
- [25] S. Koyama, et al., Adaptive resistance to therapeutic PD-1 blockade is associated with upregulation of alternative immune checkpoints, *Nat. Commun.* 7 (2016) 10501.
- [26] G. Shayan, et al., Adaptive resistance to anti-PD1 therapy by Tim-3 upregulation is mediated by the PI3K-Akt pathway in head and neck cancer, *OncoImmunology* 6 (1) (2017) e1261779.
- [27] A. Oweida, et al., Resistance to radiotherapy and PD-L1 blockade is mediated by TIM-3 upregulation and regulatory T-cell infiltration, *Clin. Cancer Res.* 24 (21) (2018) 5368–5380.
- [28] E. Limagne, et al., Tim-3/galectin-9 pathway and mMDSC control primary and secondary resistances to PD-1 blockade in lung cancer patients, *OncoImmunology* 8 (4) (2019) e1564505.
- [29] K. Sakuishi, et al., Targeting Tim-3 and PD-1 pathways to reverse T cell exhaustion and restore anti-tumor immunity, *J. Exp. Med.* 207 (10) (2010) 2187–2194.
- [30] A. de Mingo Pulido, et al., The inhibitory receptor TIM-3 limits activation of the cGAS-STING pathway in intra-tumoral dendritic cells by suppressing extracellular DNA uptake, *Immunity* 54 (6) (2021) 1154–1167 e7.
- [31] K. Jia, et al., T cell immunoglobulin and mucin-domain containing-3 in non-small cell lung cancer, *Transl. Lung Cancer Res.* 8 (6) (2019) 895–906.
- [32] Z.H. Yan, et al., Generation of mycobacterial lipoarabinomannan-specific monoclonal antibodies and their ability to identify mycobacterium isolates, *J. Microbiol. Immunol. Infect.* 54 (3) (2021) 437–446.
- [33] R.H. DeKruyff, et al., T cell/transmembrane, Ig, and mucin-3 allelic variants differentially recognize phosphatidylserine and mediate phagocytosis of apoptotic cells, *J. Immunol.* 184 (4) (2010) 1918–1930.
- [34] C.A. Sabatos-Peyton, et al., Blockade of Tim-3 binding to phosphatidylserine and CEACAM1 is a shared feature of anti-Tim-3 antibodies that have functional efficacy, *OncoImmunology* 7 (2) (2018) e1385690.
- [35] Z. Liu, et al., Study on Tim3 regulation of multiple myeloma cell proliferation via NF-kappaB signal pathways, *Front. Oncol.* 10 (2020) 584530.
- [36] M. Rezaei, et al., TIM-3 in leukemia; immune response and beyond, *Front. Oncol.* 11 (2021) 753677.
- [37] Y. Kikushige, et al., TIM-3 is a promising target to selectively kill acute myeloid leukemia stem cells, *Cell Stem Cell* 7 (6) (2010) 708–717.
- [38] Y. Kikushige, TIM-3 in normal and malignant hematopoiesis: structure, function, and signaling pathways, *Cancer Sci.* 112 (9) (2021) 3419–3426.
- [39] A.H. Wei, et al., Phase Ib study of the anti-TIM-3 antibody MBG453 in combination with decitabine in patients with high-risk myelodysplastic syndrome (MDS) and acute myeloid leukemia (AML), *Blood* 134 (Supplement 1) (2019) 570, 570.
- [40] K. Moller-Hackbarth, et al., A disintegrin and metalloprotease (ADAM) 10 and ADAM17 are major sheddases of T cell immunoglobulin and mucin domain 3 (Tim-3), *J. Biol. Chem.* 288 (48) (2013) 34529–34544.
- [41] M. Wu, et al., Soluble costimulatory molecule sTim3 regulates the differentiation of Th1 and Th2 in patients with unexplained recurrent spontaneous abortion, *Int. J. Clin. Exp. Med.* 8 (6) (2015) 8812–8819.
- [42] A.C. Anderson, et al., Promotion of tissue inflammation by the immune receptor Tim-3 expressed on innate immune cells, *Science* 318 (5853) (2007) 1141–1143.
- [43] A.K. Gandhi, et al., High resolution X-ray and NMR structural study of human T-cell immunoglobulin and mucin domain containing protein-3, *Sci. Rep.* 8 (1) (2018) 17512.
- [44] S. Schwartz, et al., Characterization of sabatolimab, a novel immunotherapy with immuno-myeloid activity directed against TIM-3 receptor, *Immunother Adv* 2 (1) (2022) Itac019.
- [45] T. Zhang, et al., Genetic mutations of tim-3 ligand and exhausted tim-3(+) CD8(+) T cells and survival in diffuse large B cell lymphoma, *J Immunol Res* 2020 (2020) 6968595.